SAND97-2578C

Mechanical Properties of Pb-Free Solder Alloys on Thick Film Hybrid Microcircuits

SAND--97-2578C

Cynthia L. Hernandez, Paul T. Vianco, Jerome A. Rejent, F. Michael Hosking
Sandia National Laboratories
Albuquerque, NM

CONF-980420--

Abstract
The technology drivers of the electronics industry continue to be systems miniaturization and reliability, in addition to addressing a variety of important environmental issues. Although the Sn-Pb eutectic alloy is widely used as a joining material in the electronics industry, it has drawn environmental concern due to its Pb content. The solder acts both as an electrical and mechanical connection within the different packaging levels in an electronic device. New Pb-free solders are being developed at Sandia National Laboratories. The alloys are based on the Sn-Ag alloy, having Bi and Au additions. Prototype hybrid microcircuit (HMC) test vehicles have been assembled to evaluate Pb-free solders for Au-Pt-Pd thick film soldering. The test components consist of a variety of dummy chip capacitors and leadless ceramic chip carriers (LCCC's). The mechanical properties of the joints were evaluated. The reflow profiles and the solid-state intermetallic formation reaction will also be presented. Improved solder joint manufacturability and increased fatigue-resistance solder alloys are the goals of these materials.[1]

Introduction

Electronic components have been surface mounted to ceramic substrates in the hybrid microelectronics industry, using printed thick film circuitry. Surface mounting meets the goals of reduced size, lower cost and increasing reliability [1]. The performance of the hybrid microcircuit (HMC) assembly is superior to that of conventional PWB assemblies, particularly at high frequencies. This is especially important for military and high-technology applications. As the technology of surface mounting has evolved, a range of packaging types became available to the HMC industry. Active components include transistors, diodes and integrated circuits (IC's) and are available in many different types of leaded and unleaded package forms. Passive components include resistors, capacitors, inductors and connectors. Resistors and some capacitors in hybrid assemblies form part of the thick-film screen printed circuit. For surface mounted assemblies, small leadless components are used.

Thick film circuitry provides the conductor paths on ceramic substrates. The thick film is screen printed to the substrate using special inks. By overprinting conductors with dielectric, a complex multilayer structure can be built up. Surface mounting components can be joined to the printed circuit board (PCB) using solder assembly. Reflow soldering is the predominant method used for joining surface mount and mixed technology assemblies and is the process used in this paper.

Although SnPb solder has been used by the electronics industry for many years for joining active and passive components, it has well documented environmental and toxicity issues. Ground water contamination by discarded electronic assemblies with Pb-bearing solders is of particular concern [2]. Several Pb-free solders have been developed over the years to address these concerns. Tin-lead eutectic solder has adequate and well-characterized physical properties including a relatively low melting point. New Pb-free alloys must meet the requirement of both a compatible melting temperature and low toxicity while maintaining good mechanical properties. This reduces the number of metals that can be considered as possible alternatives [3]. In general, Sn, with its desirable physical properties, is alloyed with other metals to produce acceptable materials. These include, Sb, Bi, Au, Cu, Ga, In, Ag and Zn. Each metal has its own specific advantages and disadvantages when used as a constituent in a solder composition. In addition, the limited solubility of a specific metal within the Sn matrix will affect performance of the solder alloy [4].

The mechanical strength of the solder depends on its microstructure. The reliability of a solder joint, therefore, depends upon its geometry and the mechanical properties of the solder alloy. It is also very dependent on the nature of the materials being joined. While the bulk strength properties of solder are relatively low, they appear greater when tested in the joint configuration of a component and a circuit board. The mechanical properties of SnPb solder and solder joints of various compositions are well documented in the literature, however, the properties of new Pb-free alloys are currently being investigated.

When two metals or alloys are in intimate contact with one another, there is an interdiffusion of one or

[1] Sandia is a multiprogram laboratory operated by Sandia Corporation, a Lockheed Martin Company, for the United States Department of Energy under Contract DE-AC04-94AL85000.

DISCLAIMER

more of the species of each alloy into the other that is temperature and time dependent [1]. In some cases, if there is a strong interaction between species, an intermetallic compound (IMC) may form. These intermetallic layers affect not only the solderability but also the mechanical properties of solder joints because they are brittle compared with solder. Since the formation and growth of brittle intermetallics along the solder/substrate interface could impact joint reliability, it is important to understand the solid state reactions [5]. Diffusion processes continue to alter the microstructure in the solid state but much more slowly than with molten solder. In the case of Sn-based alloys, they have a relatively fast solid-state reaction with elements such as Au and Cu found on the terminations of electronic components. This paper addresses these concerns as well as the mechanical properties of three Pb-free solders used on surface mount HMC assemblies.

Experimental

The hybrid test vehicle was a 96% alumina substrate with a Au-Pt-Pd thick film metallization. It measures 3.40" long x 2.50" wide x 0.040" thick. The Au-Pt-Pd film was double printed to a minimum thickness of 23μm in a repeated "print-dry-fire" procedure. A completed test vehicle is illustrated in Figure 1.

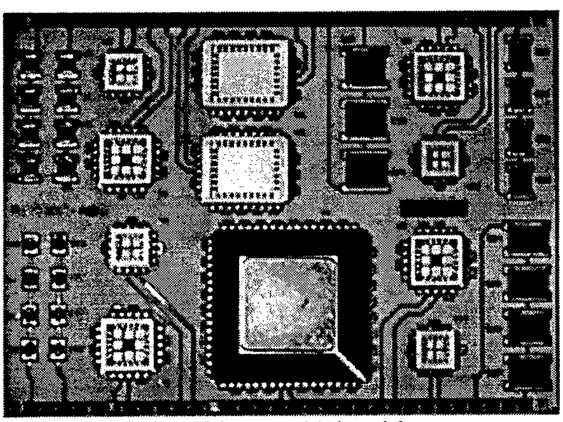

FIGURE 1. Hybrid test vehicle with components soldered in place with SnAg alloy.

The circuit design has a daisy-chained configuration to permit the measurement of electrical continuity during testing. A dielectric was deposited around the metallized features. The test components consist of a variety of dummy chip capacitors (0805, 1810, 1210, 1825 and 2225). The chip capacitors used in this study have 100% Sn terminations. The LCCC's have Au castellations with 16, 20, 32 or 68 input/outputs (I/O's) and a 50 mil pitch.

The solder compositions (expressed as wt.%) used in this study included the commercially available pastes, Sn63-Pb37 and Sn96.5-Ag3.5. The other two alloys have the composition Sn91.84-Ag3.33-Bi4.83 and Sn86.85-Ag3.15-Bi5.0-Au5.0 and were developed at Sandia National Laboratories. A differential scanning calorimeter (DSC) determined the onset temperature to be 212°C [6] and 195° for the Sn-Ag-Bi and Sn-Ag-Bi-Au alloys respectively. The precious metal additions were intended to retard the dissolution reaction between the Au-Pt-Pd thick film and the Sn constituent of the high Sn-based solders. After extensive baseline testing that included wetting, corrosion and aging experiments, several alloys were eliminated from further evaluation. The above solders demonstrated acceptable wetting and aging properties and were chosen for test vehicle assembly. Each alloy was fabricated as an ingot at Sandia and subsequently processed into a powder 30-70 microns in diameter. The powder was mixed with an RMA-based flux vehicle to form a paste with a metals content of 90%. The reflow soldering operation used in this study involves screen printing the solder paste on to the unpopulated test substrate with an 0.008" thick stencil. The components are then placed on the paste. The adhesive properties of the paste holds the components down while the board is heated to a temperature above the melting point of the given solder alloy.

A ring-in-plug test methodology was developed to determine the relative shear strength of the solder alloys. The dimensions of the individual ring and plug pieces are shown in Fig. 2.

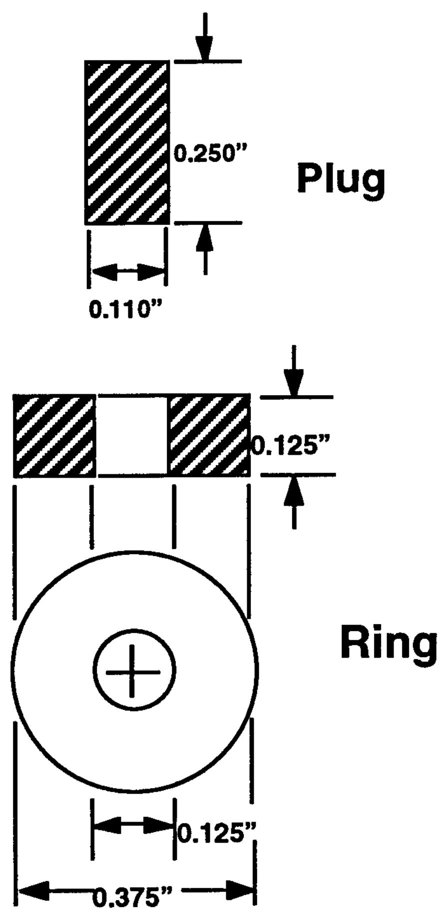

Figure 2. Ring-in-Plug test specimen geometry.

TABLE 1: Shear Data for Ring-in-Plug Test Specimens

Solder	Load (lbs.)	Stress (psi)
SnPb	269 ± 11	5840 ± 240
SnAg	367 ± 24	7970 ± 530
SnAgBi	540 ± 80	11800 ± 1700
SnAgBiAu	560 ± 15	12170 ± 330

Area = 0.046 in^2

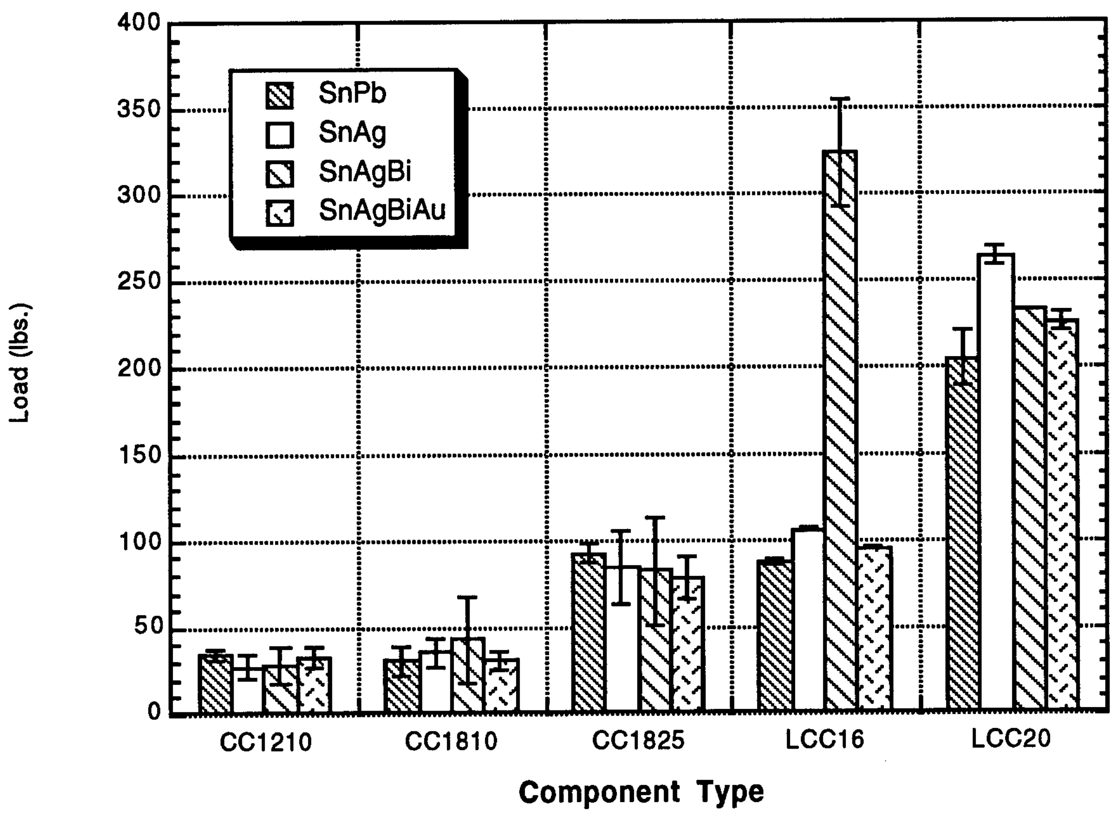

FIGURE 3. HMC Mechanical Test Data with Pre-Tinned LCC's (Load, lbs.)

Oxygen-free high conductivity (OFHC) copper was used for the ring and plug structures. The inner diameter of the ring and the outer diameter of the plug result in a solder joint gap of 0.0075 in. The sample preparation/assembly process is as follows: The ring and plug of each specimen was degreased in a solvent, etched in a 50%/HCl:50% DI water solution, rinsed and dried. Each part was then coated with an RMA flux. An annular preform of each solder alloy was placed at the juncture between the ring and plug. The entire assembly was placed on a hot plate set to a temperature of 300°C. It remained on the hot plate for a period of 20 sec. past the point at which the solder preform initially melted. The specimens were then removed from the hot plate, cooled on a chill block, and cleaned of flux residues.

Mechanical testing of the sample comprised pushing the plug through the ring. The specimens were secured into a specially designed fixture. The fixture was then placed into a load frame. The maximum recorded load was used to designate the strength of the joint. The crosshead speed was 10 mm/min. The strength data is represented by the mean and ± one standard deviation of all the measurements. This test data is shown in Table 1. The mechanical strengths of each of the Pb-free alloys are considerably higher than SnPb.

Development of Reflow Profiles

The test vehicles were processed through a tabletop solder reflow machine. The system is ideally suited for all SMT and hybrid reflow soldering applications. The unit has four conduction heat zones; all of which had to be optimized for each solder alloy. The heat zones were fully inerted with technical grade nitrogen, flowing at a rate of 30 SCFH. A sweeper bar moves the part across the heat zones at a pre-determined speed.

A time/temperature profile for complete reflow for each assembly and solder paste combination was obtained. The target parameters for this test vehicle that were used included: 1) a 1.5 to 2 min. preheat, 2) a one minute period above reflow temperature and, 3) a peak temperature 20 to 30°C above the melting point of the particular alloy to assure adequate solder reflow. Limiting factors included insufficient flux activation, solder ball formation and possible component or board damage [7]. Before populated boards with solder paste could be reflowed, bare alumina substrates with the exact same dimensions as the test vehicle were processed to develop the individual reflow profiles. Four thermocouples were attached to the substrate with high temperature tape. The board was then processed through the reflow machine. The thermocouples were read by a battery-powered temperature recording device at a data rate of five points per second. This test provided a first step in optimizing the settings. The next step was to place a few representative components on the alumina substrate. The thermocouples were again taped to the test board and processed through the reflow machine. There was a slight difference in the profiles with components on the board; the heat zone temperatures were adjusted accordingly.

The final step was to use the actual populated test vehicle to make final adjustments to the heat zone temperatures. At this point, a two-part, high temperature, high thermal conductivity epoxy system was used to bond the thermocouples to the substrate. The epoxy system gave a more representative reading of the topside temperature of the board. One thermocouple was placed under the large LCCC, one under the medium LCCC, one at the leading edge of the board and one at the trailing edge of the board. Several temperature adjustments were again required at this point due to the large heat sink of the components on the board. The final heat zone settings resulted in good reflow profiles. They are listed below in Table 2.

TABLE 2. Temperature Profiles for Each Solder Alloy

SOLDER ALLOY	REFLOW PROFILE (°C)	SWEEPER BAR SPEED (in./min.)
SnPb	126, 200, 246, 100	7
SnAg	204. 210, 266, 100	7
SnAgBi and SnAgBiAu	150, 200, 260, 100	7

Results and Discussion

After test vehicle assembly, but prior to mechanical testing, a comprehensive defect analysis was conducted under a stereo microscope to assess joint geometry, bridges, voids and component misalignment. In addition, solderability of bonding pads, formation of solder balls and thermal damage to the board were assessed. The three lead-free alloys were compared to the performance of SnPb solder.

All of the unpopulated boards exhibited excellent wetting on all of the pads. There was no bridging of joints or voids in the solder. Although, the SnAg alloy showed some solder ball formation near the LCCC pads, there was none near the chip capacitor pads. No thermal damage was observed on populated or unpopulated boards.

Test vehicles with components exhibited minimal misregistration of parts over the pads. The populated boards exhibited a variety of minor defects. In particular, the first set of boards printed with each of the four alloys showed limited solder rise up the bare Au castellations on the LCCC's. It ranged from approximately a 30% rise on the 16 I/O to 85% on the 20 I/O LCCC. However, more solder rose up the castellations on the larger package, irrespective of position. All four sides of the LCCC showed consistent behavior in this regard. The SnPb exhibited the best wetting, while the SnAgBi was the poorest. None exhibited 100% rise and the joints were very lean. This was not the case with the chip capacitors. All exhibited good wetting. After this initial observation, all subsequent LCCC's were pre-tinned with the appropriate alloy prior to assembly. All LCCC's showed much improved solder rise after pre-tinning. This was the case for all of the alloys, but the improvement was most dramatic for the SnAgBi.

There was also some non-wetting of the LCCC pads, largely at the corners. This was the case even after pre-tinning of the LCCC packages. The SnAgBiAu alloy exhibited the best wetting, followed by the SnAgBi. The SnAg alloy had the poorest pad coverage. No de-wetting was observed on any of the LCCC pads or packages for any alloy. In all cases, the chip capacitors showed good wetting of the pads and packages.

The only voids in joint fillets were observed with the SnAgBiAu alloy. These voids were very minor and appeared only on three types of chip capacitors. Although this alloy formed excellent joints, the solder appeared grainy. The SnAg alloy exhibited a greater lack of solder flow. Both the chip capacitor pads and packages had non-wetted areas.

The boards were laser sectioned without damage to any joints. Mechanical testing was then performed on representative solder joints. The board segments were introduced into a loading frame while a ram was attached to the cross head member of the load frame. At a crosshead speed of 10 mm/min., the ram pushed the component from the board. Once again, the maximum recorded load was used to designate the strength of the joint. Four tests were run per sample category. The mechanical test data for each of the alloys is illustrated in Figure 3. The strength levels of each size chip capacitor were similar for each alloy. There is, however, a slight increase in the mechanical strength of the Pb-free alloys compared to SnPb on the LCCC's.

Analysis of the solder joint microstructure began with optical images of the solder fillets. The specimens were cross sectioned in order to provide a visual inspection of the untested solder microstructure. Representative optical images of the SnAgBi solder illustrating the features of the solder joint are shown below in Figure 4.

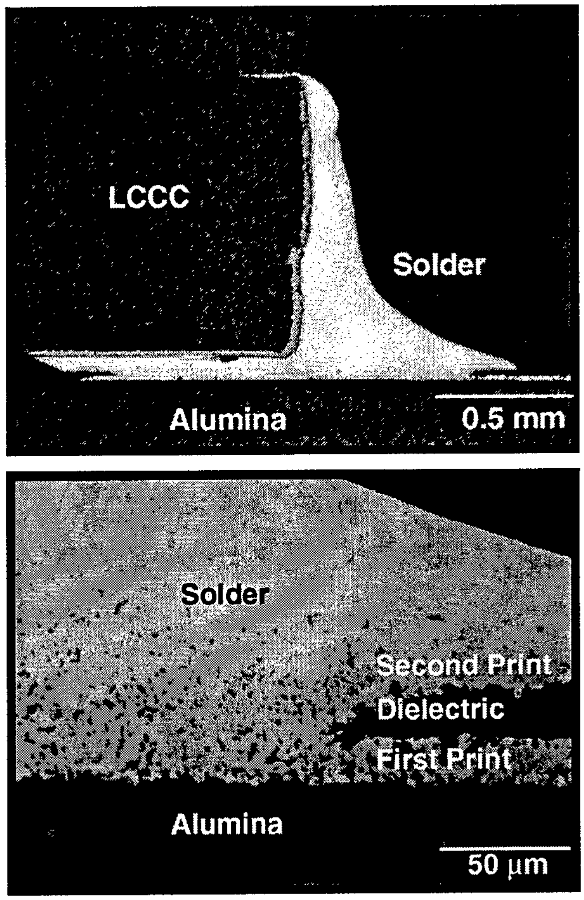

FIGURE 4. Optical images of cross-sectioned 20 I/O LCCC on the SnAgBi alloy.

Isothermal solid state aging experiments have been completed. Microstructural analysis of these samples consisted of IMC thickness measurements of parts aged from 10 to 5000 hrs. at various temperatures. The visual results of the SnPb alloy aged at 100°C are illustrated in Fig. 5. The Pb-rich phase coarsens and the growth of the intermetallic is considerable as the aging time increases. Figure 6 illustrates how quickly the intermetallic compound layer develops during solid-state aging. The SnAgBiAu system is shown at 10, 2000 and 5000 hrs. While the thick film is still visible at 10 hrs., it is consumed by 2000 hrs. Note how the microstructure of the solder quickly changes. Understanding the evolution of these structural changes is very important to the mechanical response of the joint and developing a methodology for predicting service reliability.

Conclusions

Prototype surface mount circuit boards were assembled with three Pb-free solders: SnAg, SnAgBi and SnAgBiAu. The components included four types of LCCC's and five sizes of chip capacitors. Although SnPb solder consistently yielded the best wetting and joint formation, the other Pb-free solders offer potential for component attachment in surface mount technology. Wettability of circuit board

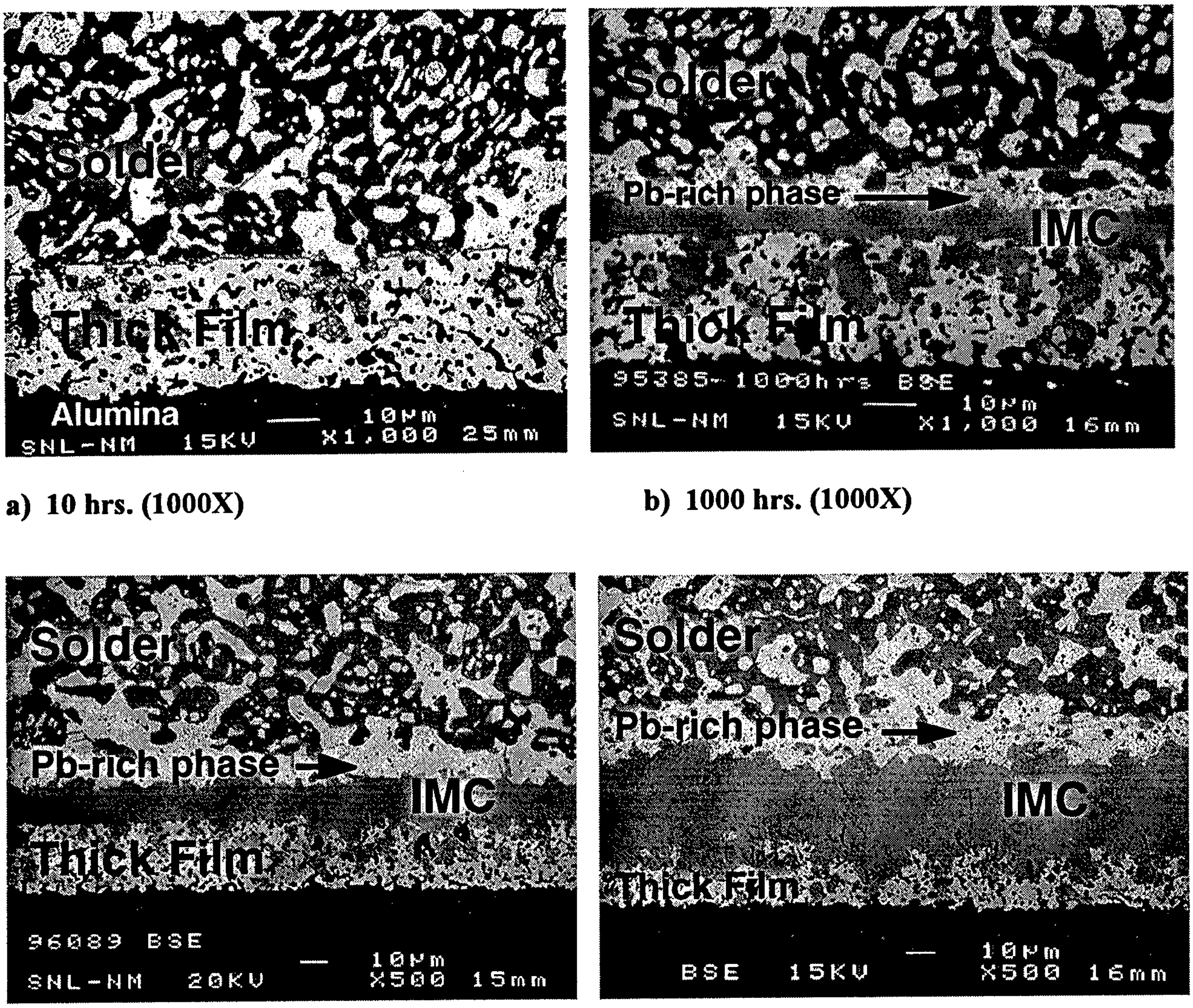

a) 10 hrs. (1000X)

b) 1000 hrs. (1000X)

c) 2000 hrs. (500X)

d) 5000 hrs. (500X)

Figure 5. Optical images of SnPb alloy aged at 100°C. Note how the Au-Pt-Pd thick film is consumed and how the IMC thickens as the part ages. The Pb-rich phase also begins to increase with time.

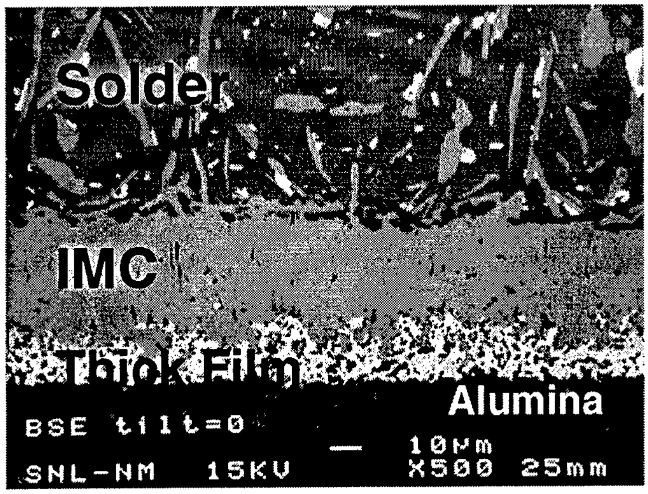

a) 10 hrs. (500X)

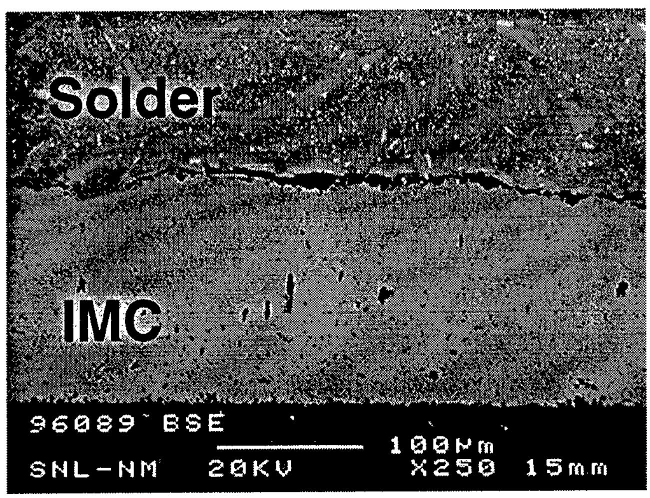

b) 2000 hrs. (250X)

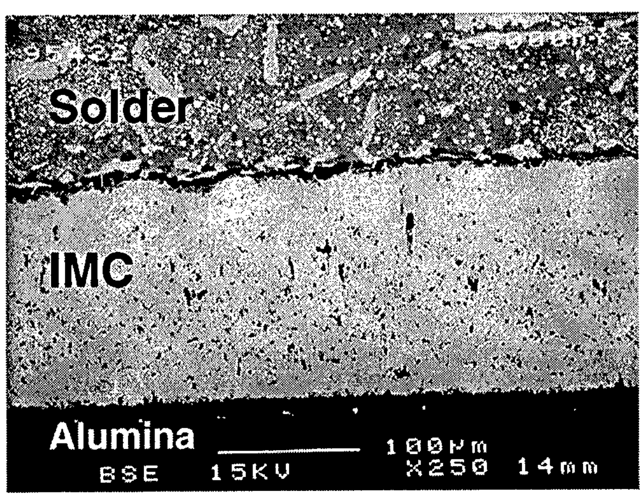

c) 5000 hrs. (250X)

Figure 6. Optical images of SnAgBiAu alloy aged at 170°C. The Au-Pt-Pd thick film is consumed much more quickly and the IMC thickness is much greater at higher temperatures.

features and packages was best with the SnAgBi alloy followed by the SnAgBiAu and SnAg systems. While the mechanical properties of the ring-in-plug were higher for the Pb-free alloys than SnPb, they were virtually the same when tested in the chip capacitor solder joints. The LCCC's printed with the Pb-free solders exhibited slightly higher mechanical strengths than those with SnPb.

Acknowledgments

The authors would like to acknowledge the efforts of James Gonzales for his help with the screen printing of the solder pastes, and Charlie Carter and Alice Kilgo for metallographic sample preparation and optical micrographs. The manuscript was reviewed by Marcelino Essien.

References

1. C. Lea, "A Scientific Guide to Surface Mount Technology", Electrochemical Publications Limited, Scotland, pp. 1, 2, 29, 66, 329, 1988.

2. Paul Vianco, Jerry Rejent, Iris Artaki, Urmi Ray, Donald Finley, Anna Jackson, "Compatibility of Lead-Free Solders with Lead Containing Surface Finishes as a Reliability Issue in Electronic Assemblies", 46th Electronic Components & Technology Conference, p.1172-1175, 1996.

3. Norbert Socolowski, "Lead-Free Alloys and Limitations for Surface Mount Assembly", Surface Mount International Proceedings (SMI, '95), p.477, 1995.

4. Ning-Cheng Lee, James A. Slattery, John R. Sovinsky, Iris Artaki, Paul T. Vianco, "A Novel Lead-Free Solder Replacement", Surface Mount International Proceedings (SMI, '94), p. 465, 1994.

5. F. M. Hosking, P. T. Vianco, J. A. Rejent, C. L. Hernandez, "Environmentally Compatible Solder Materials for Thick Film Hybrid Assemblies", ASME International Intersociety Electronic & Photonic Packaging Conference Proceedings (INTERPACK '97), p. 1364, 1997.

6. Paul T. Vianco & Chris May, "An Evaluation of Prototype Surface Mount Circuit Boards Assembled with Three Non-Lead Bearing Solders", Surface Mount International Proceedings (SMI '95), p. 482, 1995.

7. Charles L. Hutchins, "Reflow Soldering", Surface Mount Technology, pp. 32-34, 1994.

Report Number (14) SAND--97-2578C
CONF-980422--

Publ. Date (11) 19980310
Sponsor Code (18) DOE/DP, XF
UC Category (19) UC-700, DOE/ER

DOE